

# Rheological Characterization of PP/Jute Composite Melts

Smita Mohanty,<sup>1</sup> Sushil K. Verma,<sup>1</sup> Sanjay K. Nayak<sup>2</sup>

<sup>1</sup>Central Institute of Plastics Engineering and Technology, Guindy, Chennai 600032, India

<sup>2</sup>Central Institute of Plastics Engineering and Technology, Bhubaneswar-751024, India

Received 29 September 2004; accepted 20 May 2005

DOI 10.1002/app.22661

Published online in Wiley InterScience (www.interscience.wiley.com).

**ABSTRACT:** The present article summarizes an experimental study on the molten viscoelastic behavior of PP/jute composites under steady and dynamic mode. Variations in melt viscosity and die swell of the composites with an increase in shear rate, fiber loading, and coupling agent concentration have been investigated using capillary rheometer. It was observed that with the addition of fibers and MAPP, the melt viscosity of the composites increased due to improved fiber-matrix interfacial adhesion. Further, the dynamic viscoelastic behavior, measured using parallel plate rheometer, revealed an increase in the storage modulus ( $G'$ ), indicating higher stiffness in case of fiber-filled composites

as compared with the virgin matrix. Time-temperature superposition was applied to generate various viscoelastic master curves. The fiber-matrix morphology of the extrudates was also examined using scanning electron microscopy, which corroborated the findings of rheological properties. The treated composites displayed uniform distribution of fibers within the PP matrix with lesser surface irregularities. © 2005 Wiley Periodicals, Inc. *J Appl Polym Sci* 99: 1476–1484, 2006

**Key words:** jute; viscoelastic; MAPP; SEM; storage modulus

## INTRODUCTION

Fiber-reinforced thermoplastic composites have emerged as a major class of structural material in the field of aerospace, automobiles, construction etc.<sup>1</sup> These materials are characterized by easy processibility, good dimensional stability, and excellent mechanical performance.<sup>2,3</sup> The enhanced material performance primarily varies with the fiber-matrix bond strength and choice of suitable processing parameters. The processing parameters were optimized mainly by the rheological characterization of the composites. Rheological measurements conducted in various steady state and dynamic environments has been a widely used technique for determining the sensitivity of a material during processing.

Extensive studies have been carried out on the rheological behavior of short-fiber reinforced thermoplastics and elastomers.<sup>4–6</sup> The reinforcing capabilities of short fibers depend on their intrinsic mechanical properties, aspect ratio, incorporation content, fiber/matrix interaction, and processing conditions. Gupta and Purwar<sup>7</sup> have reported an increase in melt viscosities of the thermoplastics with the incorporation of glass fibers. Molden<sup>8</sup> developed a simple geometrical theory to observe the effectiveness of convergent flow in the alignment of

fibers. Advani and Tucker<sup>9</sup> proposed a tensor notation approach to describe the orientation of short fibers in polymeric matrices as the flow progresses. Similar other investigations on the flow behavior of short natural fiber reinforced composites have also been reported by several workers.<sup>10–16</sup> Studies on dynamic rheological properties of various multi-component systems provide an insight into the linear viscoelastic response of the materials. Appearance of a second plateau in the terminal region induced by agglomerated structure in various rubber particle filled systems have been investigated by Masuda et al. and Aoki and Nakayama.<sup>17,18</sup> The present article summarizes an extensive investigation on the viscoelastic behavior of PP/jute fiber reinforced composite melts both at steady and dynamic modes. A systematic study on the melt rheological properties of the matrix polymer with variable shear rates, fiber loading, and maleic anhydride grafted PP (MAPP) concentration has been made. The experimental viscosity values were compared with the theoretical predictions. Furthermore, the variation of linear viscoelastic properties of the composites at different angular frequencies has been investigated. Time-temperature superposition principle was applied to generate various viscoelastic master curves. The die swell ratio of the virgin matrix, the composites at high shear rates, and the fiber-matrix morphology of the extrudates have also been analyzed to study the effect of incorporation of jute fibers into PP matrix.

Correspondence to: S. K. Nayak (cipet\_bbsr@sify.com).

TABLE I  
Physical and Mechanical Properties of Jute Fiber

Fiber	Diameter ( $\mu\text{m}$ )	Density ( $\text{kg}/\text{m}^3$ )	Tensile strength (MPa)	Modulus (GPa)	Elongation (%)	Stiffness (GPa)	Microfibril angle ( $^\circ$ )
Jute	30	1300–1500	305	2.5–13	1.16	20–55	8

## EXPERIMENTAL

### Materials

Random copolymer of polypropylene (R120MK) with a density of  $910 \text{ kg}/\text{m}^3$  and melt flow index of  $12 \text{ g}/10 \text{ min}$ , of Reliance Industries Ltd. India, was used as the base polymer matrix.

Jute fibers having an average fiber diameter of  $20 \mu\text{m}$ , obtained from India Jute Industries Research Association (IJIRA), India, was used as reinforcing agent. The physical and mechanical properties of the fibers are listed in Table I.

Maleic anhydride grafted PP (MAPP), supplied by Eastman Chemicals Ltd. Germany, under the trade name Epolene G-3015 having  $< 1.0 \text{ wt } \%$  maleic anhydride, with  $M_w = 47,000 \text{ g}/\text{mol}$  and acid number 15, was used as coupling agent.

### Fiber treatment

The fibers were scoured in hot detergent solution (2%) at  $70^\circ\text{C}$  for 1 h to remove dirt, and core material were dried in vacuum oven at  $70^\circ\text{C}$ , and cut to 2-mm length using an electronic fiber cutting machine. These detergent washed untreated fibers were immersed in hot MAPP solution (in toluene) at  $100^\circ\text{C}$  at different concentration (1, 2%) for 5 min to obtain treated fibers.

### Composite preparation

PP/Jute composite granules at different weight percent of fibers (treated and untreated) were processed in intermeshing counter-rotating twin-screw extruder (ctw-100, Haake, Germany), having a barrel length of 300 mm and angle of entry of  $90^\circ$ . Virgin PP was fed through the hopper at the rate of  $2 \text{ kg}/\text{h}$ , and the fibers were introduced at the melting zone to minimize fiber degradation. The process was carried out at a screw speed of 45–60 rpm and a temperature difference range of 170, 175, and  $180^\circ\text{C}$  from metering to die zones. Finally, the extrudate was cooled in water at room temperature, granulated in a pelletizer (Fisons, Germany), and dried.

The composite granules along with the virgin polymer were further subjected to compression molding using Delta Malikson Pressman 100T(India), at  $170^\circ\text{C}$  to produce sheets of  $2 \pm 0.1 \text{ mm}$  thickness for various testing.

### Steady state viscosity

The variation in steady state viscosity of molten PP, untreated and treated jute filled PP composites at high shear rates ( $\dot{\gamma} > 10^3 \text{ s}^{-1}$ ) was measured using Haake torque rheometer (Haake, Germany), having a die diameter of 1 mm and L/D ratio of 15:1.5.

Compression molded disks of 25-mm diameter and 2-mm thickness were taken for the evaluation of viscosity of the materials at low shear rates ( $\dot{\gamma} = 10^{-2}$ – $10^3 \text{ s}^{-1}$ ). The measurements were performed using parallel plate rheometer (Rheometrics RDA-3, Japan) having a plate radius of 2 cm and a gap of  $1600 \mu\text{m}$ . The effect of fiber loading, shear rate, and addition of MAPP on melt viscosity  $\eta$  of the virgin matrix along with the treated and untreated composites were evaluated. In both the cases, the experiments were performed under isothermal conditions of  $170^\circ\text{C}$ .

### Die swell ratio

The extrudates obtained from the capillary die were subjected to die swell measurements with traveling microscope (Spicon, India). The diameter of the extrudates were measured after 24 h of extrusion, and the corresponding effect of shear rate, fiber loading, and addition of MAPP on the swelling behavior of PP matrix were examined.

### Interfacial properties

The surface characteristics of the extrudate were examined using scanning electron microscopy (JEOL-JSM 5800, Japan). The extrudates were fractured under liquid nitrogen and the morphology of the extrudate cross section was studied.

### Linear viscoelastic properties

The variation of linear viscoelastic properties such as storage modulus  $G'$ , loss modulus  $G''$ , complex viscosity  $\eta^*$ , and  $\tan \delta$  at variable angular frequencies ( $\omega = 10^{-2}$ – $10^3 \text{ rad}/\text{s}$ ) were investigated using the same parallel plate rheometer. Master curves of various viscoelastic functions were generated employing time-temperature superposition principle.

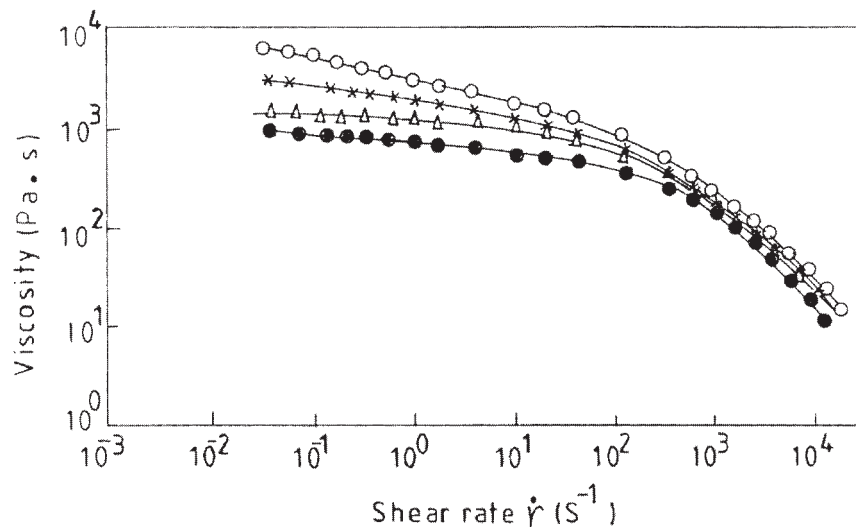


**Figure 1** Effect of fiber loading on the steady-state viscosity (●) virgin PP, (Δ) 10% PP/jute, (x) 15% PP/jute, and (o) 30% PP/jute.

## RESULTS AND DISCUSSION

### Steady-state rheological properties

#### Effect of fiber loading

The variation of steady-state viscosity ( $\eta$ ) as a function of shear rate ( $\dot{\gamma}$ ) is represented in Figure 1. The viscosity data obtained from parallel plate and capillary rheometers were combined for investigating the behavior of the materials under variable shear rates. It is evident that the viscosity of the virgin polymer increased progressively with the increase in fiber loading from 10 to 30%. This is because in the filled systems, the fibers perturb the normal flow of the polymer and hinder the mobility of the chain segments in the direction of flow.<sup>19</sup> Similar investigations have also been reported by George *et al.*<sup>15</sup> and Kalaprasad *et al.*<sup>10</sup> for pineapple leaf fiber and sisal-glass fiber hybrid LLDPE composites, respectively. In the range of low shear rates, the fibers displayed a larger reinforcing capabilities that are primarily attributed to fiber–fiber interactions, arising from weak structures made up by agglomerates of nonaligned fibers.<sup>20</sup>

The melt flow curves depicted in Figure 1 reveal that all the systems show non-Newtonian pseudoplastic behavior. In the range of high shear rates, shear-thinning behavior of the melt was observed and all the composites exhibited nearly the same viscosity. This phenomenon is probably due to alignment of the fibers at high shear rates along the tube axis, thereby decreasing the fiber to fiber collisions.<sup>21</sup> Goldsmith and Mason<sup>22</sup> have reported similar investigations and have observed radial migration of filler particles toward the capillary axis during shear flow. Thus, in a fiber-filled system the region close to the tube wall is virtually fiber free, which results in close viscosity

values of all the composites at high shear rates. The non-Newtonian pseudoplastic characteristics were further corroborated by fitting the curves obtained in the high shear rate regions in Ostwald-de-Waale or power law equation

$$\tau = K \dot{\gamma}^n$$

where  $K$  is a constant related to coefficient of viscosity and  $n$  is the flow behavior index. The values of  $K$  and  $n$  of PP and the composites at different weight percent of fiber loading, calculated by using linear regression analysis method, are shown in Table II.

As implied from the test results reported in the table, the flow behavior index  $n$  was less than one in all the cases, which further corroborates non-Newtonian pseudoplastic character of the melt. However, the degree of flow behavior index ( $n$ ) decreased with the incorporation of the fibers, and thus indicating an increase in pseudoplasticity. Conversely, the  $K$  value increased in the composites revealing an increase in the viscosity of the virgin matrix.

#### Effect of addition of MAPP

Lignocellulosic natural fibers are mostly hydrophilic in nature. This results in incompatibility with the hy-

**TABLE II**  
Effect of Fiber Loading on  $K$  and  $n$  Values

Fiber (wt %)	$K$	$n$
0	$6.07 \times 10^2$	$5.62 \times 10^{-1}$
10	$6.23 \times 10^2$	$5.01 \times 10^{-1}$
15	$6.87 \times 10^2$	$4.76 \times 10^{-1}$
30	$7.47 \times 10^3$	$4.23 \times 10^{-1}$

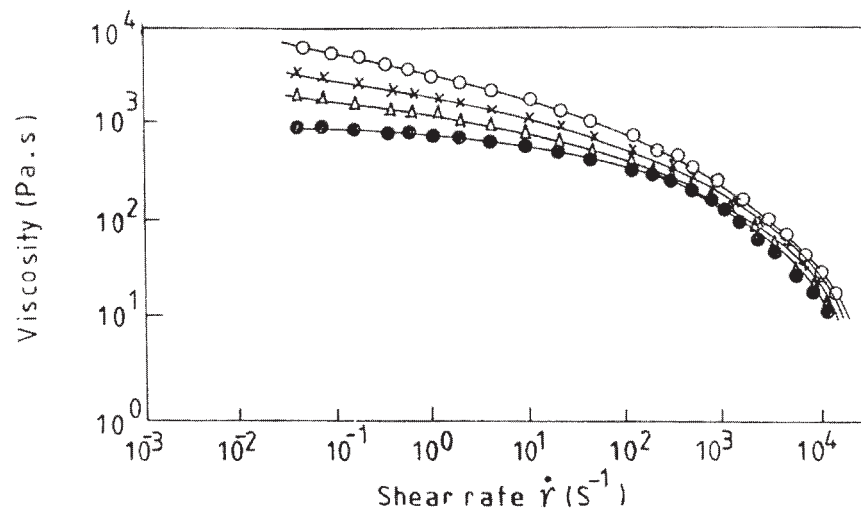


**Figure 2** Effect of addition of MAPP on steady state viscosity (●) virgin PP, (Δ) 30% PP/jute, (x) 1% MAPP, (o) 2% MAPP.

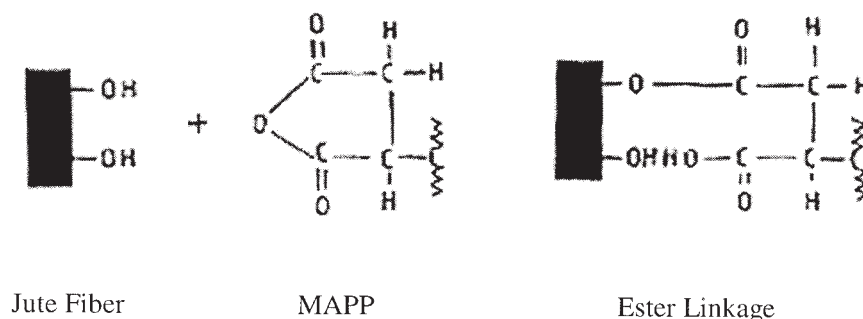
drophobic thermoplastic matrix with subsequent problems such as poor stress transfer, voids, ineffective interfaces, etc. Extensive literature survey reveals that efficient bonding between the reinforcing fibers and the polymer matrix plays a significant role on the properties of the composites. Surface modification of the fibers through various reactive additives, coupling agents, chemical reagents, light radiations, etc. has been investigated by several workers.<sup>23-28</sup> In the present study, MAPP has been used as a coupling agent to promote the fiber-matrix adhesive strength. The effect of addition of MAPP on the viscosity of PP/jute composites is represented in Figure 2. Further, a comparative account of the variation of  $\eta$  of the virgin matrix and the 30% untreated composite has also been included in the same Figure, to study the effect of surface modification.

It is evident that the viscosity of the composites increased with the addition of MAPP. This behavior is primarily attributed to improved fiber-matrix interfacial adhesion. The reaction between the jute fiber and MAPP is explained in the following reaction (Scheme 1).

The OH group of the fibers reacts with the anhydride group of MAPP forming an ester linkage. Furthermore, the PP part of MAPP adheres to the long hydrophobic PP chains of the virgin matrix, lowers the surface tension of the fibers and forms a strong interface. Additionally, the friction between the polymer and the fibers is also increased resulting in an increase in the viscosity of the composites. However, the flow curves of the treated composites also exhibited similar pseudoplastic and shear-thinning characteristics. The values of  $K$  and  $n$  derived from Ostwald-de-Waale equation showed an increase in the  $K$  value (Table III) with the addition of MAPP, thus confirming an increase in the viscosity of the melt. The degree of flow behavior index also increased, thus revealing an increase in pseudoplasticity of the treated composite melts.

#### Die swell ratio

The extrudate swell (die swell) is an indication of dimensional stability of the materials during process-



**Scheme 1** Hypothetical model of esterification reaction between the hydroxyl groups of jute fibers and anhydride rings of MAPP.

**TABLE III**  
Effect of MAPP Concentration on  $K$  and  $n$  Values

Sample type	$K$	$n$
PP virgin	$6.07 \times 10^2$	$5.62 \times 10^{-1}$
30% untreated	$7.47 \times 10^3$	$4.23 \times 10^{-1}$
1% MAPP	$8.27 \times 10^3$	$4.06 \times 10^{-1}$
2% MAPP	$8.49 \times 10^3$	$3.92 \times 10^{-1}$

ing.<sup>29</sup> As the melt emerges from the die, reorientation and recovery of the deformed molecules occur, which lead to the phenomenon of die swell. In case of composites, orientation of the polymer and the fiber takes place in the direction of flow through the capillary. The fibers and the matrix exhibit unequal retractive forces that lead to the redistribution of the fibers and recoiling effect of the polymer chains. The variation of die swell ratio  $D_e/D$  (where  $D_e$  and  $D$  are the diameters of the extrudates and die) of virgin PP, untreated, and treated composites is represented in Table IV.

It is evident that the swell ratio of the virgin matrix decreased with the incorporation of fibers. This is probably attributed to distribution of fibers within the PP matrix that results in stress transfer from matrix to the fiber, thereby retarding the elastic recovery of the material.<sup>29</sup> Further, the treated composites displayed a lesser die swell, and thus confirming enhanced fiber-matrix adhesive strength. However, the swell ratio increased with the shear rate, which is probably due to decrease of normal stress and elastic recovery at low shear rates.

### Extrudate morphology

The SEM micrographs of the extrudate surfaces of untreated and treated composites at 30% fiber loading are depicted in Figures 3a–3d, respectively.

It is evident that at higher shear rate of  $150 \text{ s}^{-1}$  (Fig. 3(b)), the surface irregularities were more prevalent, with randomly distributed untreated fibers within the matrix. However, at low shear rate of  $15 \text{ s}^{-1}$  (Fig. 3(a)) the extrudate surface was comparatively smooth, thus revealing the shear sensitivity of the materials.

The surface characteristics of MAPP treated composites (Figs. 3c and 3d) displayed uniform distribution of fibers within the matrix. This further confirms efficient fiber-matrix interfacial bond strength with the addition of MAPP.

### Linear viscoelastic properties

The melt state linear viscoelastic properties were investigated using parallel plate rheometer. A time-dependent oscillatory strain was applied with a variable frequency between  $10^{-2}$  and  $10^3 \text{ rad/s}$ . The linearity of the measurements was confirmed by repeating the

experiments at high and low strain amplitudes and observing the independence of measured storage and loss moduli.

The frequency-dependent viscoelastic properties (storage modulus  $G'$ , loss modulus  $G''$ , and  $\tan \delta$ ) obtained at different temperatures were superposed by the application of time-temperature superposition principle to prepare viscoelastic master curves. Both frequency shift factors  $a_T$  (horizontal) and modulus shift factors  $b_T$  (vertical) were applied simultaneously to create master curves. Depending on the experimental temperature and reference temperature, the frequency shift factors were fitted to the WLF equation

$$\log a_T = -c_1(T-T_0)/c_2 + (T-T_0)$$

Where  $c_1(3.36)$  and  $c_2(17.07)$  are constants and  $T_0$  is the reference temperature ( $130^\circ\text{C}$ ). The rheological master curves based on linear viscoelastic measurements for the virgin matrix, untreated, and treated composites are represented in Figures 4–6, respectively.

It is evident that the curves reveal three distinct regions: glassy, plateau, and terminal, respectively, when going from high to low frequency zones.<sup>30</sup> The virgin matrix displays a characteristic viscoelastic response of an well entangled polymer with a crossover frequency of  $3 \text{ rad/s}$ , below which it displays liquid like relaxation<sup>31</sup> (Fig. 4).

In the glassy region, where the deformation frequency is high compared with the average relaxation time of the polymer chain, the chains cannot adjust quickly enough to dissipate the applied stress, thereby resulting in high modulus. As implied from Figures 4(a) and 5(a), the rigidity of the matrix polymer increased with the incorporation of untreated jute fibers, over the entire range of explored frequency, which resulted in an increase in  $G'$ . Furthermore, the crossover region in the untreated composites was obtained at a marginally higher frequency in comparison with the virgin matrix, thus revealing a lesser relaxation time of polymer chains in the composites.

The plateau region revealed a relatively constant storage modulus from frequency range of  $10^{-1}$  to  $10^{-2} \text{ rad/s}$ , indicating that the PP chains have sufficient time to relax locally. The magnitude of  $G''$  also increased in the untreated composite.

**TABLE IV**  
Die Swell Ratio of Virgin PP, Untreated, and Treated PP/Jute Composites at 30% Fiber Loading

Sample type	Shear rate ( $\text{s}^{-1}$ )	
	15	150
Virgin	1.21	1.38
Untreated	1.19	1.35
Treated	1.16	1.33



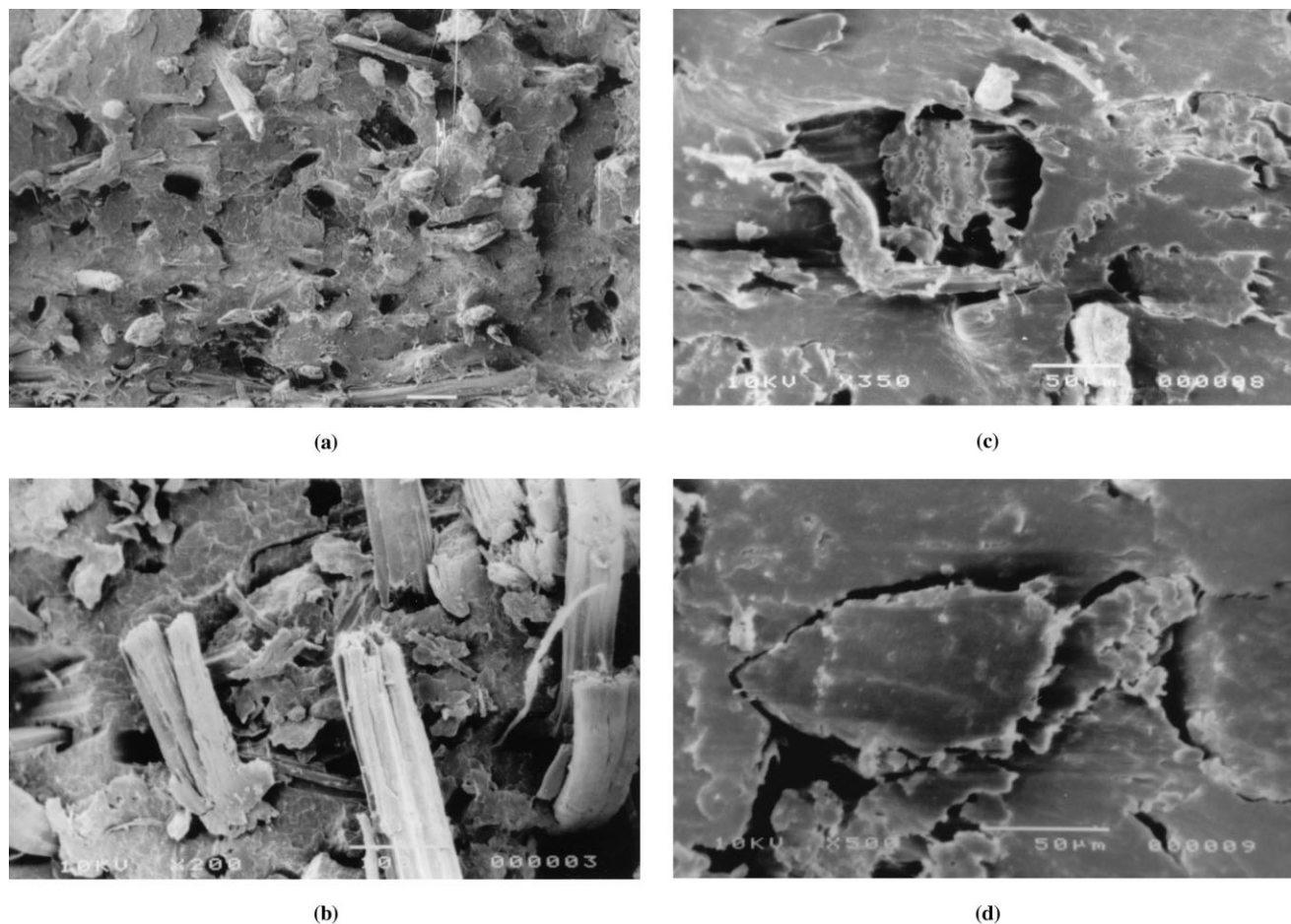


**Figure 3** (a) SEM micrograph of untreated composite at 30% fiber loading and shear rate of  $15 \text{ s}^{-1}$ . (b) SEM micrograph of untreated composite at 30% fiber loading and shear rate of  $150 \text{ s}^{-1}$ . (c) SEM micrograph of treated composite at 30% fiber loading and shear rate of  $15 \text{ s}^{-1}$ . (d) SEM micrograph of treated composite at 30% fiber loading and shear rate of  $150 \text{ s}^{-1}$ .

Conversely, the viscoelastic master curve of the MAPP treated composites (Figs. 6(a) and 6(b)) exhibited a comparatively higher magnitude of  $G'$  and  $G''$ , and thus indicating enhanced fiber-matrix interfacial adhesion in presence of MAPP. The crossover frequency was also obtained in the similar range as the untreated composite. Further, the frequency dependence of high frequency relaxation behavior in the composites was virtually unaffected by the addition of MAPP, suggesting that the observed chain relaxation modes remain unaltered with the presence of MAPP.

Additionally, in the terminal region where the time allowed for relaxation is longer than the longest relaxation time in the polymers, the melt behaves like a viscoelastic liquid with  $G''$  proportional to  $\omega$ . In all the cases  $G'$  exceeds  $G''$  beyond the crossover zone. In the range of low frequencies (*i.e.*,  $\omega \leq 0.1 \text{ rad/s}$ ), both the treated as well as untreated composites exhibit nearly frequency independent  $G'$  and  $G''$ , and thus suggesting the possibility of pseudosolid like behavior at long times owing to incomplete relaxation of the chains in the composites.<sup>6</sup>

The frequency dependence of  $\tan \delta$  for virgin PP, untreated, and treated composites is represented in Figures 4(c), 5(c), and 6(c), respectively. It is evident that the magnitude of  $\tan \delta$  increased with the addition of fibers and MAPP. This shows that the viscous dissipation of the PP increases in the composites.

The variation of complex viscosity  $\eta^*$  as a function of angular frequency  $\omega$  is enumerated in Figures 4(d), 5(d), and 6(d), respectively. It is observed that  $\eta^*$  of the virgin matrix along with the treated and untreated composites decreased linearly with an increase in the angular frequency, thus showing pseudoplastic characteristics. All the systems displayed non-Newtonian behavior over the entire range of frequency, with the treated composite having maximum magnitude of  $\eta^*$ .

Thus in all the cases, the viscoelastic functions are in agreement with the principle of time-temperature superposition.  $G'$  and  $G''$  increased monotonically at all frequencies that are analogous to other filled systems.<sup>31</sup>

Linear viscoelastic master curves were generated with the application of both frequency ( $a_T$ ) as well as

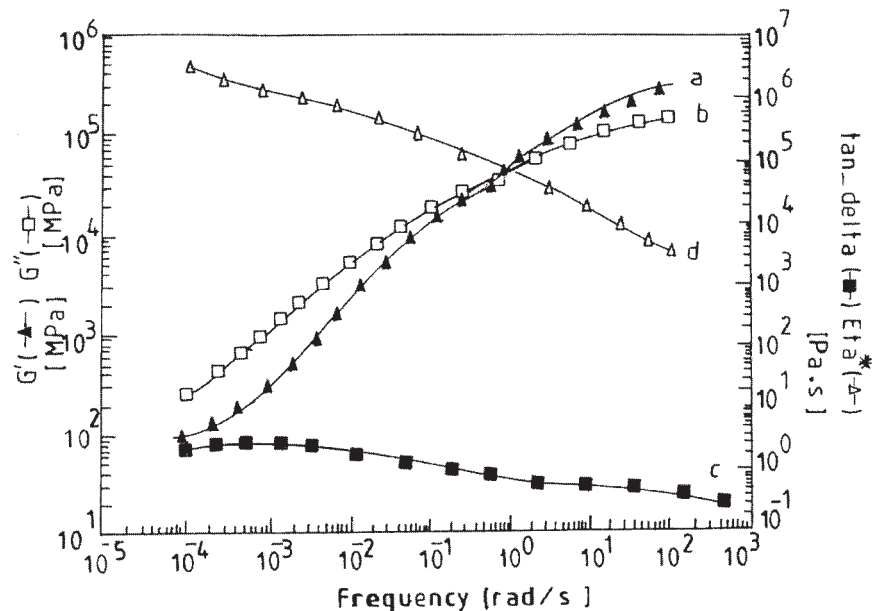


Figure 4 Linear viscoelastic master curves of virgin PP.

modulus shift factors ( $b_T$ ). For all the samples, a small temperature dependent  $b_T$  was employed ( $0.9 \leq b_T \leq 1.1$ ) to generate time-temperature superposed master curves.

The variation of  $a_T$  and  $b_T$  as a function of temperature is graphically represented in Figure 7. As observed from the Figure,  $a_T$  values are nearly independent of fiber loading and addition of MAPP,

and are similar to those of the virgin matrix. This indicates that the temperature dependence of the relaxation probed is similar in the composites as well as in the virgin matrix.<sup>6</sup> The fibers incorporated into the bulk matrix do not have temperature-dependent relaxation, as a result of which there was almost negligible contribution to the observed  $a_T$  values.

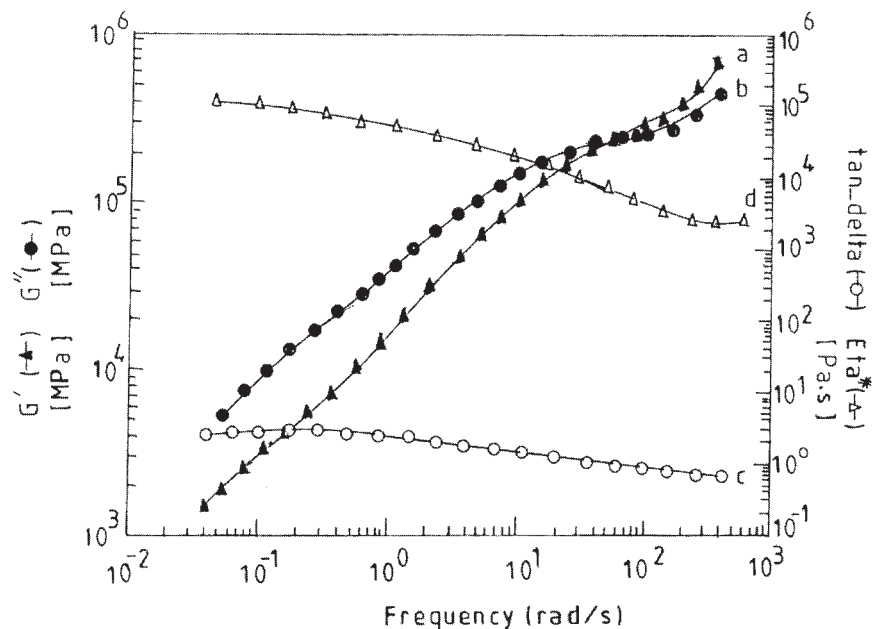


Figure 5 Linear viscoelastic master curves of untreated PP/jute composite at 30% fiber loading.

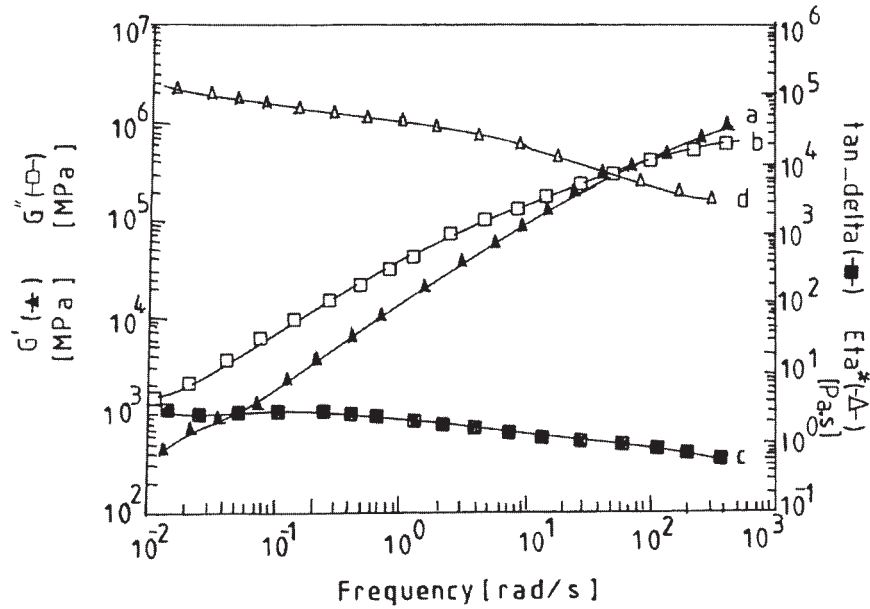


Figure 6 Linear viscoelastic master curves of treated PP/jute composite at 30% fiber loading and 2% MAP.

CONCLUSIONS

The molten viscoelastic behavior of jute fiber-reinforced PP composites was studied as a function of shear rate, angular frequency, fiber loading, and MAPP concentration. The steady-state viscosity of the composites increased with the incorporation of fibers. The composites treated with MAPP showed enhanced viscosity values due to improved fiber-

matrix adhesion. All the composites exhibited pseudoplastic characteristics that can be represented by power law equation. The swelling ratio of the HDPE, however, decreased in the composites. Further, the dynamic properties ( $G'$ ,  $G''$ ,  $\eta^*$ , and  $\tan \delta$ ) also increased with reinforcement. The morphology of the extrudates revealed efficient fiber-matrix adhesion in the treated composites.

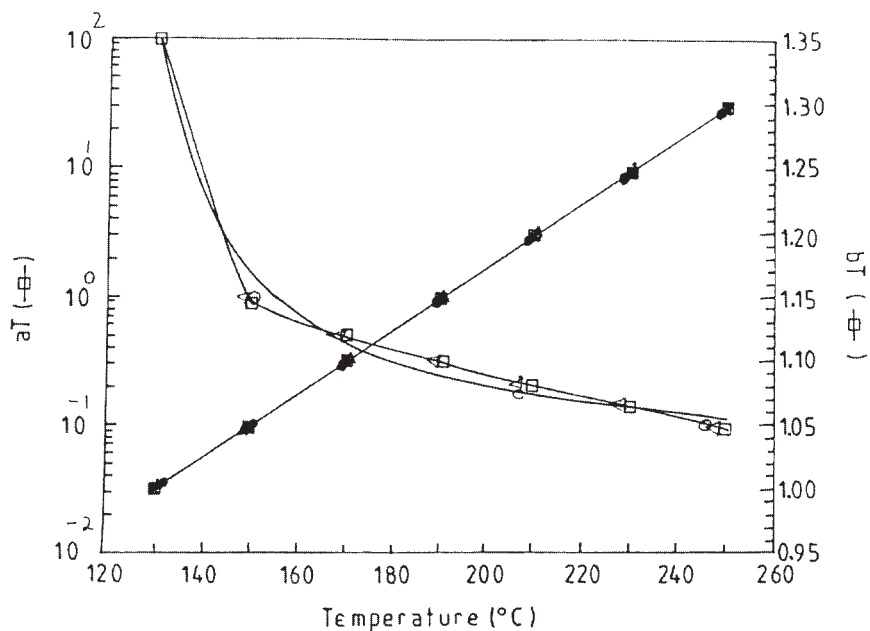


Figure 7 Frequency and modulus shift factors for virgin PP (●), untreated (Δ), and treated (145) PP/jute composites (open symbols for  $a_T$  and closed symbols for  $b_T$ ).



**References**

1. Ma, C. C. M. First Asian–Australian Conference on Composite Materials, ACCM-I, Osaka, Japan, 1998; p 205.
2. Laun, H. M.; Coll, J. *Interface Sci* 1984, 262, 257.
3. Ghosh, T.; Grmela, M.; Carreau, P. J. *Polym Compos* 1995, 16, 144.
4. Wu, G.; Song, Y.; Zheng, Q.; Du, M.; Zhang, P. *J Appl Polym Sci* 2003, 88, 2160.
5. Liang, J. Z.; Li, R. K. Y. *J Reinforc Plast Compos* 1999, 18, 1077.
6. Yurekli, K.; Krishnamoorti, R.; Tse, M. F.; Mcelrath, K. O.; Tsou, A. H.; Wang, H. C. *J Polym Sci* 2001, 39, 256.
7. Gupta, A. K.; Purwar, S. N. *J Appl Polym Sci* 1985, 30, 934.
8. Molden, G. F. *J Mater Sci* 1969, 4, 283.
9. Advani, S. G.; Tucker, C. L. *J Rheol* 1987, 31, 751.
10. Kalaprasad, G.; Mathew, G.; Pavithran, C.; Thomas, S. *J Appl Polym Sci* 2003, 89, 432.
11. Kalaprasad, G.; Thomas, S. *J Appl Polym Sci* 2003, 89, 443.
12. Varghese, S.; Kuriakose, B.; Thomas, S.; Premaletha, C. K.; Koshy, A. T. *Plast Rubber Compos Process Appl* 1993, 20, 93.
13. Varghese, S.; Kuriakose, B.; Thomas, S.; Premaletha, C. K. *Plast Rubber Compos Process Appl* 1994, 21, 238.
14. Geethamma, V. G.; Janardhan, R.; Ramamurthy, K.; Thomas, S. *Int J Polym Mater* 1996, 32, 147.
15. George, J.; Janardhan, R.; Anand, J. S.; Bhagawan, S. S.; Thomas, S. *Polymer* 1996, 37, 5421.
16. Aurich, T.; Mennig, G. *Int J Plast Technol* 2002, 5, 9.
17. Masuda, T.; Kitamura, M.; Onogi, S. *J Rheol* 1981, 25, 453.
18. Aoki, Y.; Nakayama, K. *Polym J* 1982, 14, 951.
19. Crowson, R. J.; Folkes, M. J.; Bright, P. F. *Polym Eng Sci* 1980, 20, 63.
20. Carneiro, O. S.; Maia, J. M. *Polym Compos* 2000, 21, 960.
21. Crowson, R. J.; Folkes, M. J. *Polym Eng Sci* 1980, 20, 934.
22. Goldsmith, S. C.; Mason, S. G. In *Rheology Theory and Application*; Eirich, F. R., Ed.; Vol. 4; Academic Press: New York, 1967.
23. Mohanty, S.; Verma, S. K.; Nayak, S. K.; Tripathy, S. S. *Int J Plast Technol* 2003, 7, 75.
24. Mishra, H. K.; Dash, B. N.; Tripathy, S. S.; Padhi, B. N. *Polym Plast Technol Eng* 2000, 39, 187.
25. Mohanty, A. K.; Khan, M. A.; Hinrichen, G. *Composites: Part A* 2000, 31, 143.
26. Rana, A. K.; Basak, R. K.; Mitra, B. C.; Lawther, M.; Banerjee, A. N. *J Appl Polym Sci* 1997, 64, 1517.
27. Gassan, J.; Bledzki, A. K. *Composites: Part A* 1997, 28A, 1001.
28. Karmakar, A. C.; Hoffmann, A.; Hinrichen, G. *J Appl Polym Sci* 1994, 54, 1803.
29. Chiu, W. Y.; Hsueh, T. C. *J Appl Polym Sci* 1986, 32, 4663.
30. Zhao, J.; Hahn, S. F.; Hueul, D. A.; Meunier, D. M. *Macromolecules* 2001, 34, 1737.
31. Khan, S. A.; Prud'homme, R. K. *Rev Chem Eng* 1987, 4, 205.